Thermal behavior of Functionally Graded Materials

Daikh Ahmed Amine, Megueni Abd El Kader
Department of Mechanical Engineering
Djelali Liabes University, Faculty of Technology
Sidi Bel Abbes, Algeria
daikh.ahmed.amine@gmail.com

Abstract— **Mathematical expressions have been used to find thermal behavior of functionally graded plate. Temperature distributions are used on the basis of three different types to evaluate the thermal properties of FGMs. Material properties are vary continuously through the thickness according to a power law function, exponential function, and sigmoid function in terms of the volume fraction of the constituents. The computational mathematical software *Matlab.R2014b* has been used to carry out the numerical calculations and the graphs been plotted using *OriginLab.9*.**

Keywords—Functionally graded materials; Material properties; Temperature distribution.

I. INTRODUCTION

In recent years, *functionally graded materials* (FGMs) have gained considerable importance in extremely high temperature environments such as nuclear reactors and chemical plants. FGMs are also considered as a potential structural material for the future high-speed spacecraft [1]. FGMs are composite materials, microscopically inhomogeneous, in which the mechanical properties vary smoothly and continuously from one surface to the other. This is achieved by gradually varying the volume fraction of the constituent materials. This continuous change in composition results in graded properties of FGMs. These novel materials were first introduced by a group of scientists in Sendai, Japan, in 1984 [1, 2]. Typically, these materials are made from a mixture of ceramic and metal or a combination of different metals. The advantages of using these materials are that they are able to withstand high-temperature gradient environments while maintaining their structural integrity. The ceramic constituent of the material provides the high-temperature resistance due to its low thermal conductivity. The ductile metal constituent, on the other hand, prevents fracture caused by stresses due to high-temperature gradient in a very short period of time. Further, a mixture of a ceramic and a metal with a continuously varying volume fraction can be easily manufactured [2-6]. This eliminates interface problems and thus the stress distributions are smooth. FGMs were initially designed as thermal barrier materials for aerospace structural applications and fusion reactors. FGMs are now developed for general use as structural elements in extremely high temperature environments. A listing of different applications can be found in [7]. The continuous changes in their microstructure distinguish FGMs from the conventional laminated composite materials. Fiber-matrix composites have a mismatch of mechanical properties across an interface due to two discrete materials bonded together. As a result, the constituents of the fiber-matrix composites are prone to debonding at extremely high thermal loading. Further, cracks are likely to initiate at the interfaces and grow into weaker material sections. Additional problems include the presence of residual stresses due to the difference in coefficients of thermal expansion of the fiber and matrix in the composite materials. These problems can be resolved by gradually varying the volume fraction of the constituents rather than abruptly changing them across an interface. This gradation in properties of the material reduces thermal stresses, residual stresses, and stress concentration factors [8]. Furthermore, the gradual change of mechanical properties can be tailored to different applications and working environments. This makes FGMs preferable in many applications.

FGMs show great promise in applications where operating environments are challenging, including spacecraft heat shields, heat exchanger tubes, turbine blade, engine components, biological implant, wear resistant bulk material and coating, graded bandgap semiconductor and high power electrical contacts or even magnets. One of the main applications of FGMs is as thermal barrier coatings (TBCs) at high temperatures. FGM TBCs have been proved to have the abilities to optimize temperature field, reduce thermal stress and enhance thermal resistance. A SiC/C FGM thermal barrier coating for a combustion chamber has been developed for a Japanese space shuttle [9]. Repeated hot gas flow tests indicated that the FGM thermal barrier coating has high resistance to delamination and cracking at high temperatures. ZrO_2/Ni FGM was used as TBC for a rocket engine [10] . No delamination was observed after 550 seconds of combustion. ZrO_2 stabilized with Y_2O_3 FGM was used as TBC for turbine blades [11]. It showed outstanding erosion and thermal shock resistance.

The static and dynamic responses of plates in thermal environment have widely been studied. Some current researches assume temperature-independent material

properties and uses simple rule of mixtures to estimate material properties at different positions, in order to simplify their calculations, but these assumptions ignore temperature effects as well as microscopic particle interactions and thus can be unrealistic.

In other hand, Cho and Ha [12] conducted volume fraction optimizations for minimizing the thermal stress of FGMs in a constant thermal distribution. Shen [13] employed a mixed Galerkin-perturbation technique to analyze the nonlinear bending of FGM plates subjected to a transverse load and in uniform thermal environments. Tounsi et al. [14] and Hamidi et al. [15] studied the bending response of FGM sandwich plates under both thermal and thermo mechanical loading conditions. Bouderba et al. [16] used a refined plate theory to investigate the thermo mechanical bending response of functionally graded plates resting on Winkler-Pasternak elastic foundations. A thermal buckling and post-buckling analysis was presented by Shen [17] , Thornton [18], Eslami et al. [19], Matsunaga [20], Zhao et al. [21] and Liew et al. [22]. Pradhan and Murmu [23] presented a thermo-mechanical vibration analysis of an FGM sandwich beam using differential quadrature method. One may also see [24, 25, 26, 27, 28, 29] (and also the literature herein) to find study related with the application of thermal or temperature environment on vibration analysis of functionally graded plates. In this study, material properties of FGMs are evaluated under different types of temperatures distribution.

II. MATHEMATICAL MODELING

II.1 Material properties

The functionally graded material (FGM) can be produced by continuously varying the constituents of multi-phase materials in a predetermined profile. The most distinct features of an FGM are the non-uniform microstructures with continuously graded properties. An FGM can be defined by the variation in the volume fractions. Most researchers use the power-law function, exponential function, or sigmoid function to describe the volume fractions. This paper also uses FGM plates with power-law, exponential, or sigmoid function. For analysis of FGM structures, three main functions can be employed.

A. Exponential function: E-FGM

To describe the material properties, the exponential function is used [30]

$$P(z) = P_2 e^{B(z+\frac{h}{2})} \qquad (1)$$

$$B = \frac{1}{h}.ln(\frac{P_1}{P_2})$$

where h is the thickness of the plate and $P(z)$ denotes a generic material property such as modulus, P_1 and P_2 indicate the property of the top and bottom faces of the plate, respectively.

B. Power-law function: P-FGM

The volume fraction of the P-FGM is assumed to obey a power-law function

$$V_1(z) = \left(\frac{h/2+z}{h/2}\right)^n \qquad (2)$$

Where n is the material parameter that dictates the material variation profile through the thickness. Once the local volume fraction $V(z)$ has been defined, the material properties of a P-FGM can be determined by the rule of mixture [31]

$$P(z) = V(z).P_1 + [1 - V(z)].P_2 \qquad (3)$$

C. Sigmoid function: S-FGM

The volume fraction using two power-law functions which ensure smooth distribution of stresses is defined.

for $-h/2 \le z \le 0$

$$V_1(z) = \frac{1}{2}\left(\frac{h/2+z}{h/2}\right)^n \qquad (4)$$

for $0 \le z \le h/2$

$$V_1(z) = 1 - \frac{1}{2}\left(\frac{h/2-z}{h/2}\right)^n \qquad (5)$$

By using the rule of mixture, the material properties of the S-FGM can be calculated by

for $-h/2 \le z \le 0$

$$P(z) = V_1(z).P_1 + [1 - V_1(z)].P_2 \qquad (6)$$

for $0 \le z \le h/2$

$$P(z) = V_2(z).P_1 + [1 - V_2(z)].P_2 \qquad (7)$$

The material P-FGM and S-FGM will be metal-rich when the power index $n = \infty$, and ceramic-rich in $n = 0$.

II. 2 Thermal analysis

A FG rectangular plate of side a x b and thickness h, made from a mixture of ceramic and metal, is considered in this paper. It is assumed that the composition is varied so that the top surface of the plate ($z = h/2$) is ceramic-rich, whereas the bottom surface ($z = -h/2$) is metal rich. Therefore the material properties of the plate, the Young's modulus $E(z, T)$, the mass density $\rho(z, t)$, coefficient of thermal expansion $\alpha(z, T)$ and thermal conductivity $K(z, T)$ vary through the depth (z).

The constituents of the FGM plate are assumed to be ZrO_2 as material 1 and Ti-6Al-4V as material 2. ZrO_2 ceramic have

low thermal conductivity, which give them high thermal resistance. Titanium alloy Ti-6Al-4V is a light material with high strength. The elastic modulus E, Poisson's ratio v, thermal conductivity k, specific heat C, coefficient of thermal expansion α and density ρ are assumed to be temperature-dependent [32, 33, 34] and can be expressed as a function of temperature as

$$P(T) = P_0(P_{-1}T^{-1} + 1 + P_1T + P_2T^2 + P_3T^3) \quad (8)$$

where $T = T_0+\Delta T(z)$, T_0=300K (ambient or free stress temperature), ΔT is the temperature change, P_i (i = -1, 0, 1, 2, 3) are the temperature dependent coefficients which can be seen in the table of materials properties (Table 1).

The temperature variation is assumed to occur in the thickness direction only and one dimensional temperature field is assumed to be constant in the plane of the plate. In this paper many types of thermal boundary condition are applied.

A. Uniform temperature rise

The initial uniform temperature of the plate is assumed to be T_0 (T_0 = 300K). The temperature field is expressed as

$$T = T_0 + \Delta T \quad (9)$$

where ΔT denotes the temperature change.

B. Linear temperature rise

Assuming the temperature T_m and T_c at the bottom and top of the plate, the temperature field under linear temperature rise in z direction is expressed as

$$T(z) = T_c + \Delta T\left(\frac{z}{2}+\frac{1}{2}\right), \quad \Delta T = T_c - T_m \quad (10)$$

C. Nonlinear temperature rise

In this case we use two types of thermal boundary condition.

Thermal condition-I

It is assumed that one value of the temperature is imposed on the upper surface and the other value on the lower surface. In this case, the temperature distribution along the thickness can be obtained by solving a steady-state heat transfer equation through the thickness of the plate. The equation for the temperature through the thickness is given by

$$-\frac{d}{dz}\left(k(z)\frac{dT}{dz}\right) = 0 \quad (11)$$

where the thermal conductivity $k(z)$ is assumed to be independent to the temperature. This equation is solved by imposing boundary condition of $T = T_0+T_c$ at $z = h/2$ and $T = T_0+T_m$ at $z = -h/2$. The solution of this equation

$$T(z) = T_0 + \Delta T(z) \quad (12)$$

for the isotropic material plate, the temperature rise through the thickness is

$$\Delta T(z) = \frac{T_c + T_m}{2} + \frac{T_c - T_m}{h}z \quad (13)$$

Table. 1. Temperature-dependent coefficients of Young's modulus $E(Pa)$, Poisson's ratio v, thermal expansion coefficients $\alpha(1/K)$, mass density $\rho(kg/m^3)$ and thermal conductivity $K(W/mK)$ [35].

Material	**P_{-1}**	**P_0**	**P_1**	**P_2**	**P_3**
ZrO2					
E	0	244.27e+9	-1.37 e-3	1.214e-6	-3.681e-10
v	0	0.3	0	0	0
α	0	12.766e-6	-1.491e-3	1.006e-5	-6.778e-11
ρ	0	3000	0	0	0
K	0	6.10	0	0	0
Ti-6Al-4V					
E	0	122.56e+9	-4.586e-4	0	0
v	0	0.30	0	0	0
α	0	7.5788e-6	6.638e-4	-3.147e-6	0
ρ	0	4429	0	0	0
K	0	1.78	0	0	0
Si_3N_4					
E	0	348.43e+9	-3.07 e-4	2.16 e-7	-8.946 e-11
v	0	0.24	0	0	0
α	0	5.87e-6	9.095 e-4	0	0
ρ	0	2370	0	0	0
K	0	9.19	0	0	0
SUS304					
E	0	201.04e+9	3.079e-4	-6.543 e-7	0
v	0	0.3262	-2.002 e-4	3.797 e-7	0
α	0	12.33e-6	8.086 e-4	0	0
ρ	0	8166	0	0	0
K	0	12.04	0	0	0

for an P-FGM and E-FGM plates

$$\Delta T(z) = T_m + \frac{T_c - T_m}{\int_{-h/2}^{h/2}(dz/k(z))}\int_{-h/2}^{z}(dz/k(z)) \tag{14}$$

and for an S-FGM plate

$-h/2 \le z \le 0$;

$$T(z) = T_m + \frac{T_{mp} - T_m}{\int_{-h/2}^{0}(dz/k(z))}\int_{-h/2}^{z}(dz/k(z)) \tag{15}$$

$0 \le z \le h/2$;

$$T(z) = T_{mp} + \frac{T_c - T_{mp}}{\int_{0}^{h/2}(dz/k(z))}\int_{0}^{z}(dz/k(z)) \tag{16}$$

where T_{mp} is the temperature at mid-plane of the plate.

In the case of power-law (P-FGM) and sigmoid function (S-FGM), the solution to (14), (15-16) also can be expressed by means of polynomial series

for P-FGM

$$T = T_m + \frac{T_c - T_m}{R}\sum_{i=0}^{e}\left|\frac{1}{in+1}\left(\frac{1}{2}+\frac{z}{h}\right)^{in+1}\left(\frac{-k_{cm}}{k_m}\right)^{i}\right|$$
$$R = \sum_{i=0}^{e}\left|\frac{1}{in+1}\left(\frac{-k_{cm}}{k_m}\right)^{i}\right| \tag{17}$$

where k_c , k_m denote the thermal conductivity of ceramic surface and metal surface respectively, and k_m $k_{cm} = k_c - k_m$.

for S-FGM

$-h/2 \le z \le 0$;

$$T = T_{mp} + \frac{T_c - T_{mp}}{R}\sum_{i=0}^{e}\left|\frac{1}{in+1}\left|\frac{\frac{h}{2}+z}{h}\right|^{in+1}\left(\frac{-k_{cmr}}{2k_{mp}}\right)^{i}\right|$$
$$R = \sum_{i=0}^{e}\left|\frac{1}{in+1}\left(\frac{-k_{cm}}{2k_m}\right)^{i}\right| \tag{18}$$

$0 \le z \le h/2$;

$$T = T_m + \frac{T_{mp} - T_m}{R}\sum_{i=0}^{e}\left|\frac{1}{in+1}\left|\frac{\frac{h}{2}-z}{h}\right|^{in+1}\left(\frac{k_{mpr}}{2k_{mp}}\right)^{i}\right|$$
$$R = \sum_{i=0}^{e}\left|\frac{1}{in+1}\left(\frac{k_{mpr}}{2k_{mp}}\right)^{i}\right| \tag{19}$$

where T_{mp} and k_{mp} are the temperature and the thermal conductivity of mid-plane of the plate, $k_{cmp} = (k_c - k_m)/2$ and $k_{mpm} = (k_{mp} - k_m)/2$.

Thermal condition-II

It is assumed that the lower surface was held at a prescribed temperature $T(z) = T_0 + \Delta T(z)$ and the heat flow from the upper surface to the lower one is assumed to be q (W/m^2). The heat transfer rate per unit area (heat flux) q is proportional to the normal temperature rise

$$q = -k(z)\frac{dT(z)}{dz} \tag{20}$$

Solving this equation, we have the same temperature equation expressed in (9). For an isotropic material plate with constant thermal conductivity, the temperature rise through the thickness is

$$\Delta T(z) = T_m + \frac{q}{k}\left(\frac{h}{2}+\frac{q}{k}z\right) \tag{21}$$

For a P-FGM plate with the thermal conductivity varying through the thickness, the temperature rise through the thickness is

$$\Delta T(z) = T_m + q\int_{-h/2}^{z}(dz/k(z)) \tag{22}$$

and for S-FGM

$$\Delta T(z) = T_m + q\int_{-h/2}^{z}(dz/k(z)),\ -h/2 \le z \le 0 \tag{23}$$

$$\Delta T(z) = T_{mp} + q\int_{-0}^{z}(dz/k(z)),\ 0 \le z \le h/2 \tag{24}$$

III. RESULT AND DISCUSSION

We consider that a FGM plate has the ceramic at the heated surface $z = h/2$ and the metal at the cooled surface $z = -h/2$ and their compositions vary continuously in the thickness direction of the plate. The material properties are taken into consideration the temperature dependency for the temperature range of $0 \le T \le 800°C$. The FGM plate is made of titanium alloy (Ti–6Al–4V) on its lower surface and zirconium oxide (ZrO_2) on its upper surface. In this analysis, we take that the temperature on the surface 100% metal equal to zero. We evaluate in this work only Young modulus and coefficient of thermal expansion because the influence of temperature on Young modulus E and coefficient of thermal expansion α is very large and important than Poisson's ratio υ and Density ρ.

Figure 1 presents Young modulus for P-FGM, S-FGM and E-FGM through the thickness plate. Figure 2 shows the linear thermal expansion as a function of temperature for several materials. The change of thermal expansion is relatively small for Si3N4 and SUS304. The temperature has a strong effect on the thermal expansion of Ti-6Al-4V and ZrO_2, where the thermal expansion α of Ti-6Al-4V decreases as temperature T increases, while α increases with T in ZrO_2.

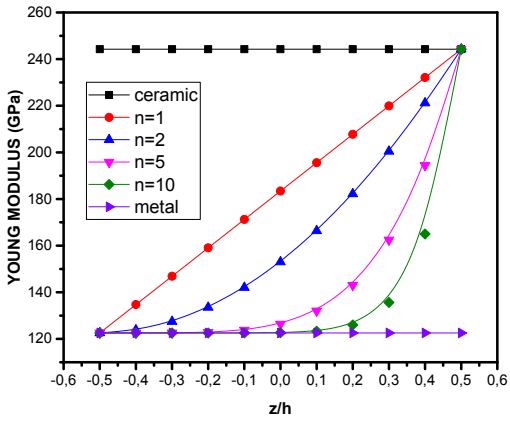

P-FGM

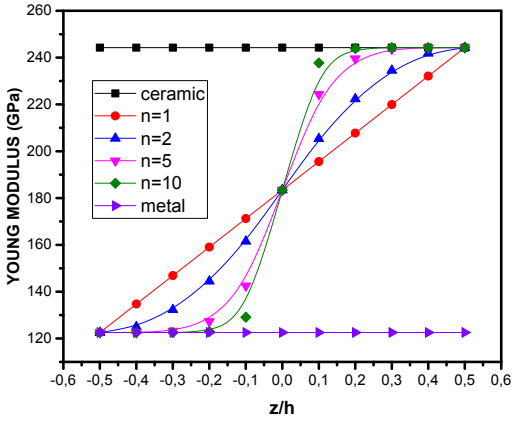

S-FGM

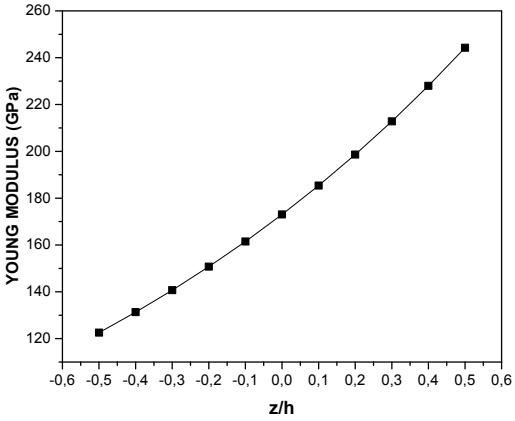

E-FGM

Fig. 1. The effective modulus of FGM plate.

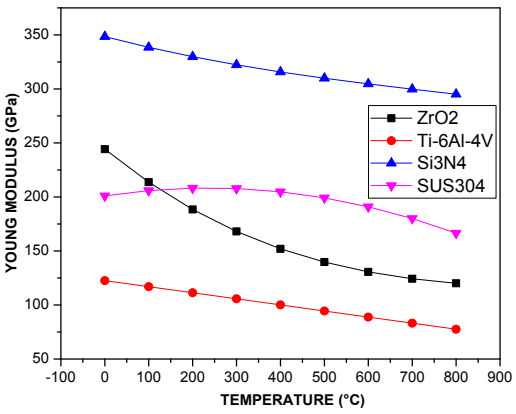

(*a*)

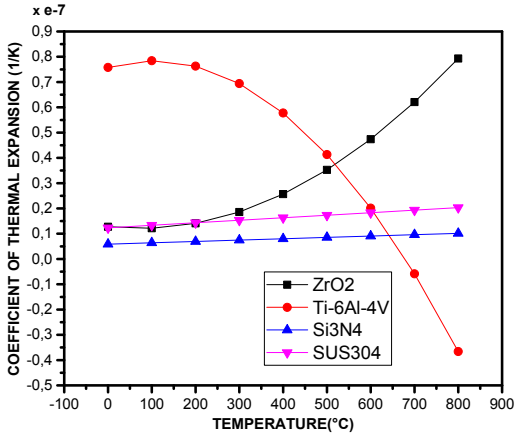

(*b*)

Fig. 2. Material properties as a function of temperature. (*a*) Young modulus, (*b*) Coefficient of thermal expansion.

Figure 3 shows the variation of elastic modulus E of P-FG plates with the volume fraction index n. figure 3 (*a*) indicates elastic modulus of plate on temperature $\Delta T=0$, figure 3 (*b*) on nonlinear temperature rise with $\Delta T = 500°C$, figure 3 (*c*) on linear temperature rise with $\Delta T = 500°C$, and figure 3 (*d*) on uniform temperature rise with $\Delta T = 500°C$.

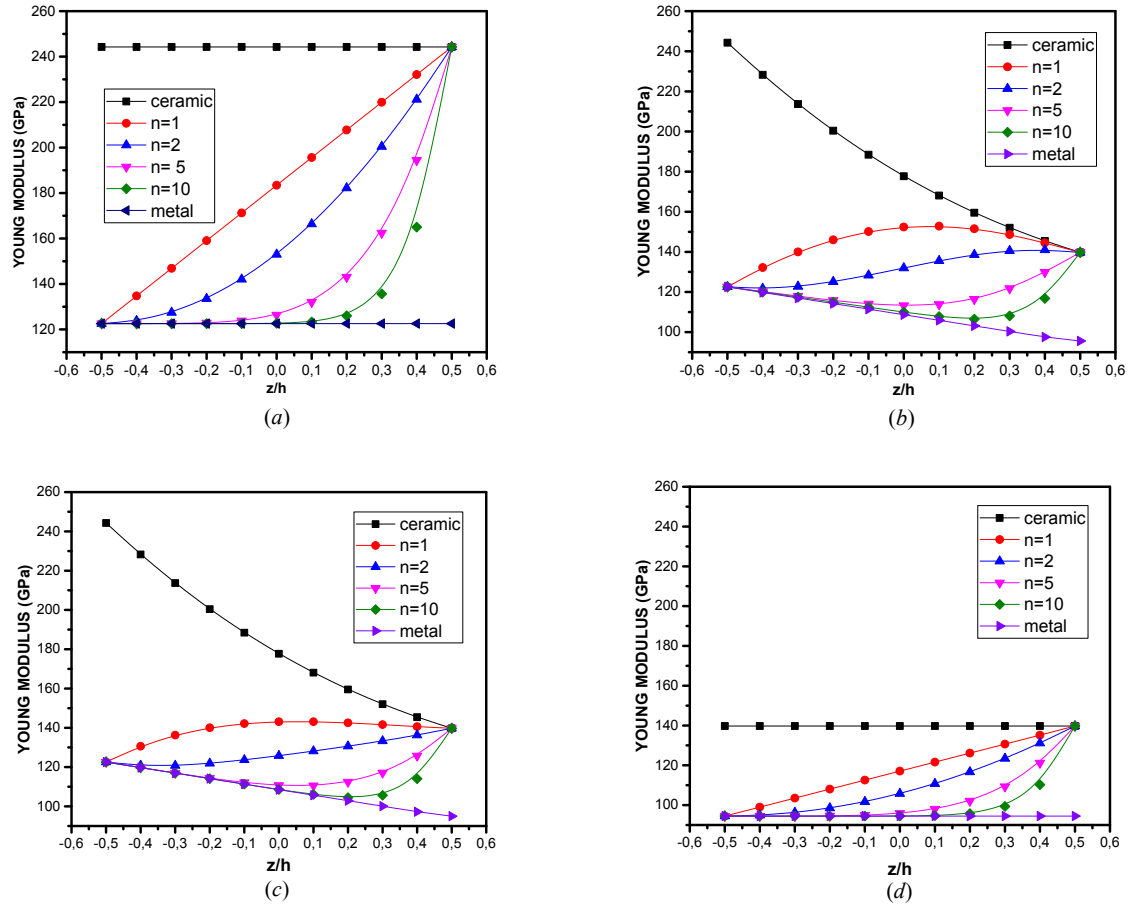

Fig. 3. The variations of Young modulus of P-FG plate along the thickness direction.
(*a*) T=0°C, (*b*) Nonlinear temperature rise T=500°C,(*c*) Linear temperature rise T=500°C, (*d*) Uniform temperature rise T=500°C.

For the plate on temperature ΔT=0, elastic modulus varies large away from the lower surface according to volume of ceramic. However, elastic modulus variations have a different from those of above two cases as shown in figure 3 (b) and (c). In the case of uniform temperature, the variation of young modulus in ΔT=500 take a same form of ΔT=0, with large change of values. The rate of decrease of Young modulus for $n > 1$ is high compared to $n = 1$.

Figure 4 and 6 presents the variation of coefficient of thermal expansion along the thickness of P-FG and S-FG plate with different value of index *n*.

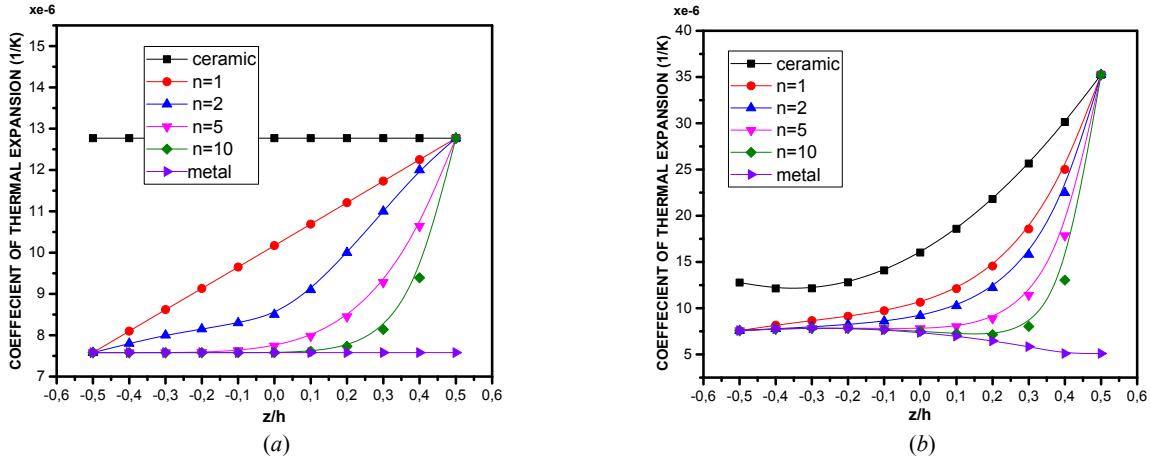

Fig. 4. The variations of coefficient of thermal expansion of P-FG plate along the thickness direction.
(*a*) T=0°C, (*b*) Nonlinear temperature rise T=500°C.

The nonlinear temperature distribution along the thickness of S-FG plate is complicated and difficult to obtain because of the unknown temperature value of mid-plane T_{mp}. This temperature takes a value less than the average value between temperature upper surface and lower surface $(T_{mp} < (T_c-T_m)/2)$. For this reason, we analyze the material properties of S-FG plate with linear and uniform temperature rise only (Figure 5).

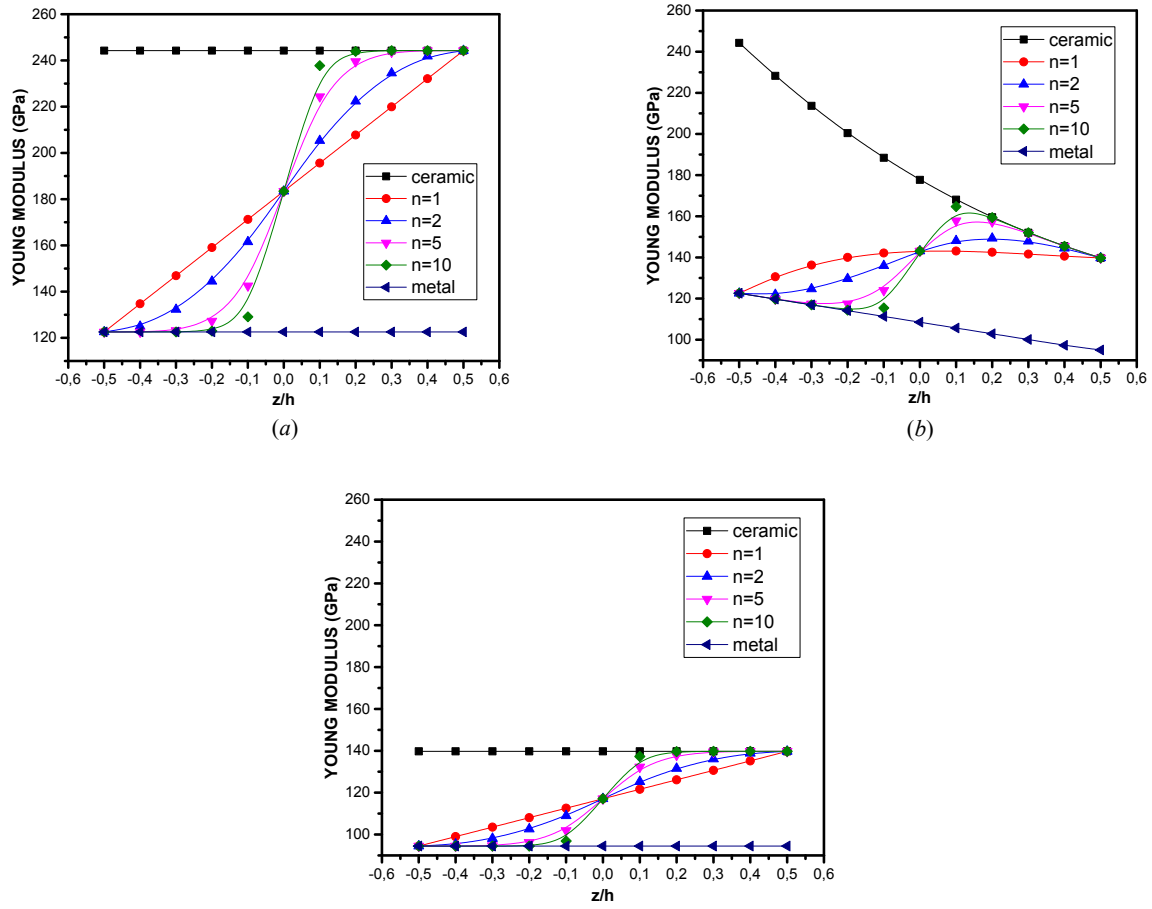

(*a*) (*b*)

(*c*)

Fig. 5 The variations of Young modulus of S-FG plate along the thickness direction.
(*a*) T=0°C , (*b*) Linear temperature rise T=500°C , (*c*) Uniform temperature rise T=500°C.

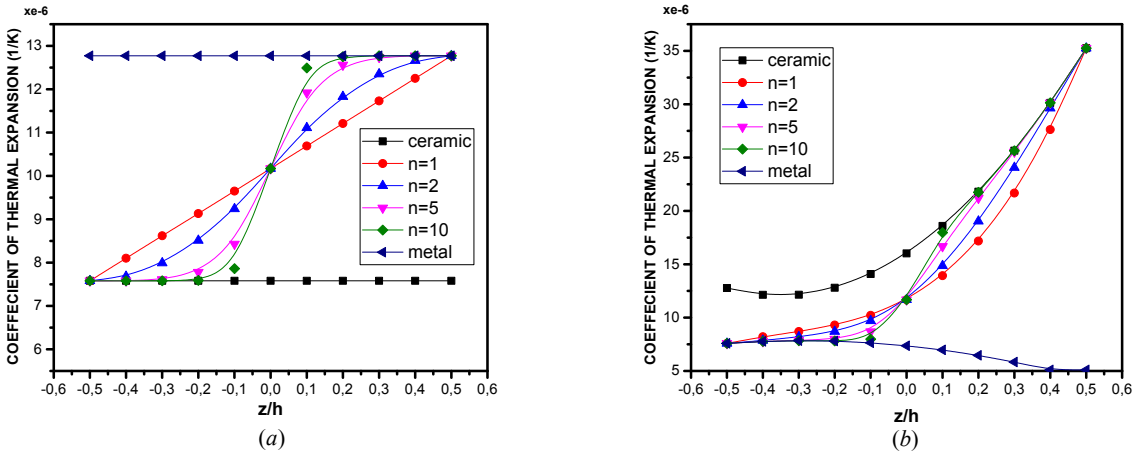

(*a*) (*b*)

Fig. 6 The variations of coefficient of thermal expansion of S-FG plate along the thickness direction.
(*a*) T=0°C, (b) Linear temperature rise T=500°C.

Figure 7, 8 and 9 depicts the effect of the temperature on the elastic modulus of P-FG plate, S-FG plate, and E-FG plate. As we can observe, for each material E decreases as the temperature increases. These results indicate the large effect of high temperature on the response of engineering structures.

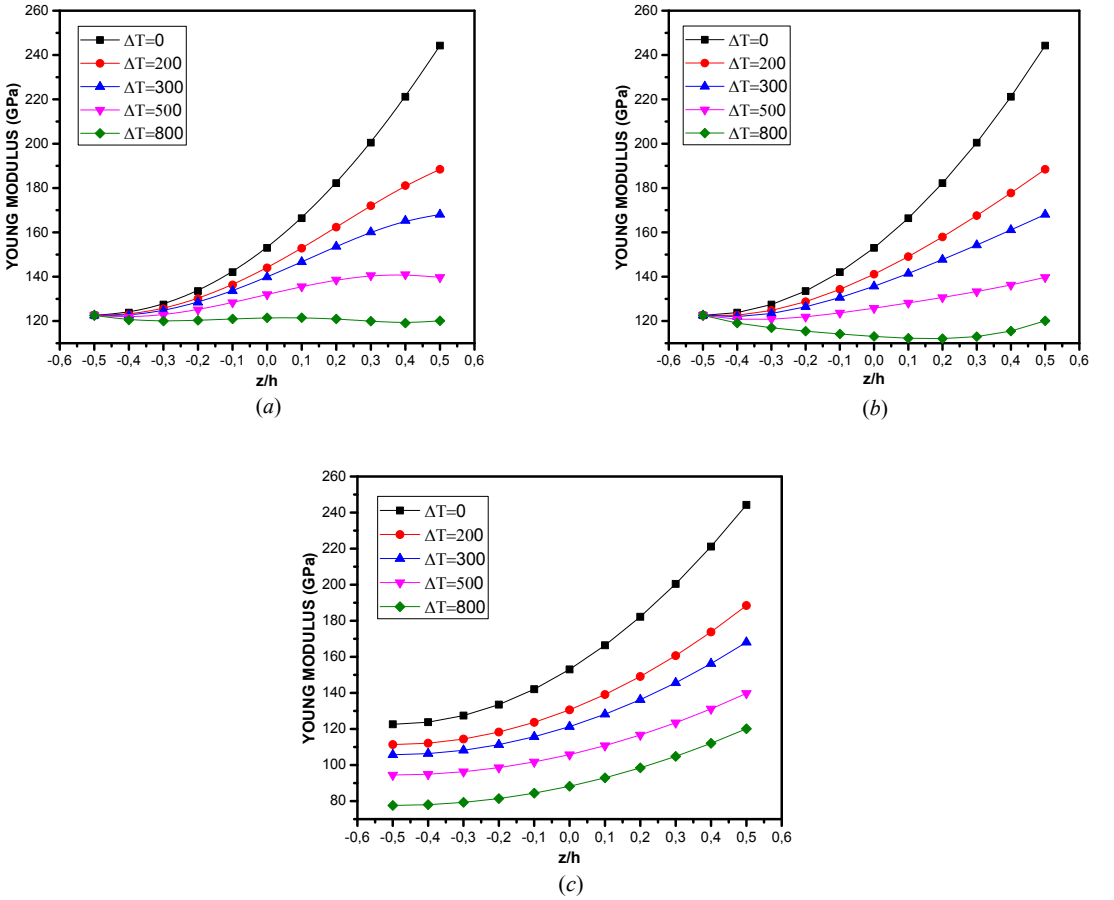

(*a*) (*b*)

(*c*)

Fig. 7. Young modulus of P-FG plate along the thickness direction with Temperature changes ($n=2$).
(*a*)Nonlinear temperature rise, (*b*) Linear temperature rise, (*c*) Uniform temperature rise.

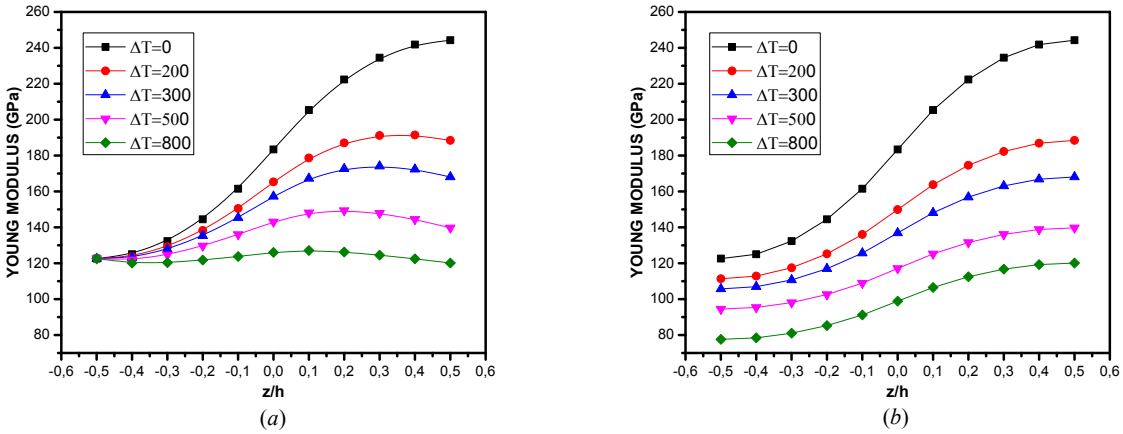

(*a*) (*b*)

Fig. 8 Young modulus of S-FG plate along the thickness direction with Temperature changes ($n=2$).
(*a*) Linear temperature rise, (*b*) Uniform temperature rise.

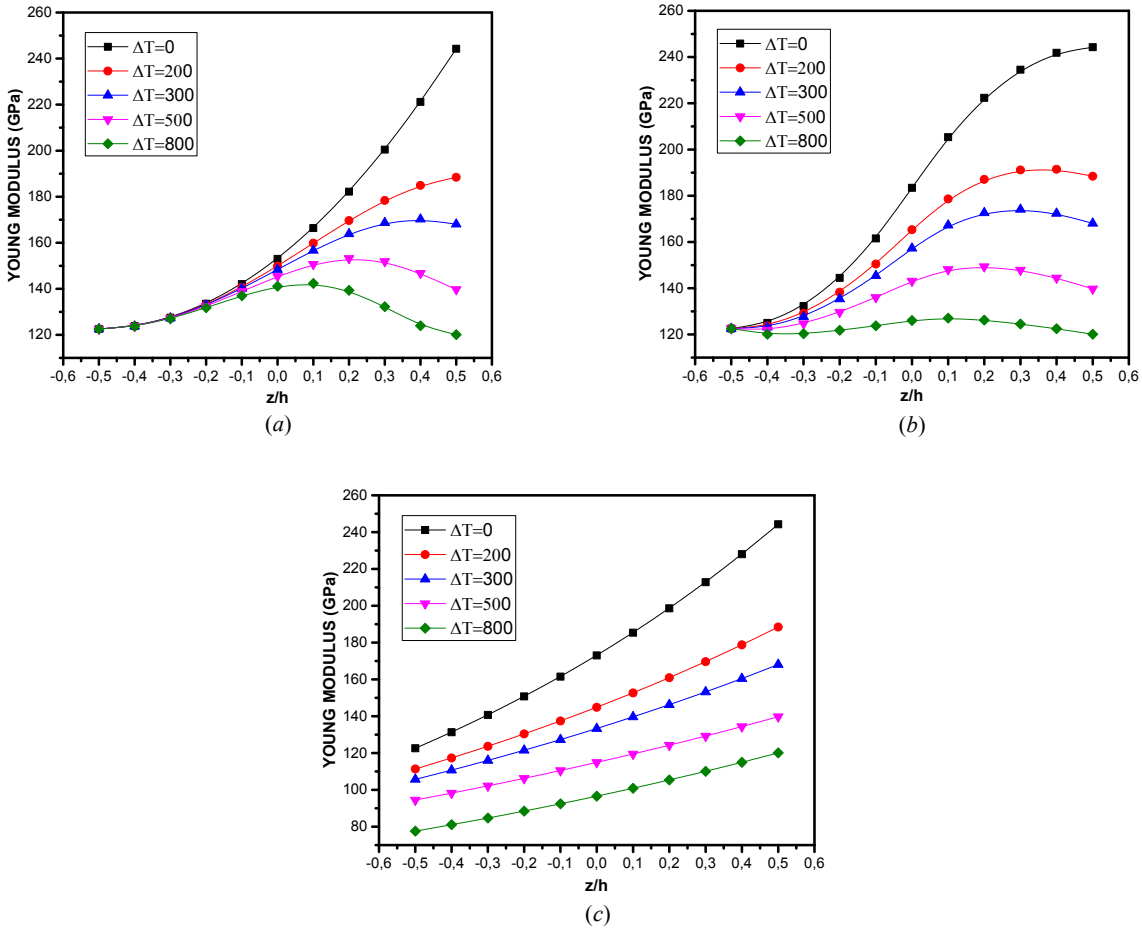

Fig. 9. Young modulus of E-FG plate along the thickness direction with Temperature changes.
(*a*)Nonlinear temperature rise, (*b*) Linear temperature rise, (*c*) Uniform temperature rise.

IV. Conclusion

In this study, Calculations were made to determine the influence of the changes of temperature distribution on elastic material properties .the elastic properties of materials (modulus of elasticity, and coefficient of thermal expansion) vary with temperature. The power index of FGMs can be defined as a coefficient of isolation of FGMs. The high temperatures change completely the properties of FGMs.

These results are the first step to investigate temperature dependent static and dynamics behavior of functionally graded structures.

References

[1] M. Yamanouchi, M. Koizumi, T. Hirai, and I. Shiota (eds.), Proc. First Int. Sympos. Functionally Gradient Materials, Japan, 1990.

[2] M. Koizumi, The Concept of FGM, Ceramic Trans., Functionally Gradient Materials, vol. 34, pp. 3-10, 1993.

[3] N. Sata, Characteristic of SiC-TiB2 Composites as the Surface Layer of SiC-TiB2-Cu Functionally Gradient Material Produced by Self-Propagating High-Temperature Synthesis, Ceramic Trans., Functionally Gradient Materials, vol. 34, pp. 109-116, 1993.

[4] H. Yamaoka, M. Yuki, K. Tahara, T. Irisawa, R. Watanabe, and A. Kawasaki, Fabrication of Functionally Gradient Material by Slurry Stacking and Sintering Process, Ceramic Trans., Functionally Gradient Materials, vol. 34, pp. 165-172, 1993.

[5] B. H. Rabin and R. J. Heaps, Powder Processing of Ni-Al203 FGM, Ceramic Trans., Functionally Gradient Materials, vol. 34, pp. 173-180, 1993.

[6] Y. Fukui, Fundamental Investigation of Functionally Gradient Material Manufacturing System Using Centrifugal Force, Int. J. Japan Soc. Mech. Engrs. Set, III, vol. 34, pp. 144-148, 1991.

[7] FGM Forum, Survey for Application of FGM, The Society of Non-Tradition Technology, Tokyo, Japan, 1991.

[8] F. Erdogan and M. Ozturk, Diffusion Problems in Bonded Nonhomogeneous Materials with an Interface Cut, Int. J. Engrg. Sci., vol. 30, pp. 1507-1523, 1992
[9] Tada, Y. (1995). Space and aerospace vehicle components.
[10] Y Kuroda, K. K., A Moro, M Togawa. (1991). Evaluation tests of ZrO2/Ni functionally gradient materials for regeneratively cooled thrust engine applications. Ceramic Transactions, 34, Proc, of The Second Int'l Symp. on FGM'92, American Ceramic Society, 289-296.
[11] G. W. Goward , D. A. G., R.C. Krutenat. (1994).
[12] J.R. Cho, D.Y. Ha, Volume fraction optimization for minimizing thermal stress in Ni–Al2O3 functionally graded materials, Materials Science and Engineering A 334 (2002) 147–155.
[13] H.S. Shen, Nonlinear bending response of functionally graded plates subjected to transverse loads and in thermal environments, International Journal of Mechanical Sciences 44 (2002) 561–584.
[14] Tounsi A, Houari M.S.A, Benyoucef S, Bedia Adda. A refined trigonometric shear deformation theory for thermoelasti cbending of functionally graded sandwich plates. Aerospace Science and Technology2013;24:209–20.
[15] Hamidi A, Zidi M, Houari M.S.A, Tounsi A. ,A new four variable refined plate theory for bending response of functionally graded sandwich plates under thermomechanical loading. Composites: Part B 2012(inpress).
[16] Bouderba B, Houari MSA, Tounsi A. Thermomechanical bending response of FGM thick plates resting on Winkler–Pasternak elastic foundations. Steeland Composite Structures2013; 14:85–104.
[17] Shen H-S. Postbuckling of FGM plates with piezoelectric actuators under thermo-electro-mechanical loadings. International Journal of Solids and Structures 2005;42:6101–21.
[18] Thornton EA. Thermal buckling of plates and shells. Appl Mech Rev 1993;46:485–506.
[19] Shariat BAS, Eslami MR. Thermal buckling of imperfect functionally graded plates. Int J Solids Struct 2006;43:4082–96.
[20] Matsunaga H. Thermal buckling of functionally graded plates according to a 2 D higher-order deformation theory. Compos Struct 2009;90:76–86.
[21] Zhao X, Lee YY, Liew KM. Mechanical and thermal buckling analysis of functionally graded plates. Compos Struct 2009;90:161–71.
[22] Liew KM, Yang J, Kitipornchai S. Thermal postbuckling of laminated plates comprising functionally graded materials with temperature dependent properties. ASME Journal of Applied Mechanics 2004;71:839–50.
[23] Pradhan SC, Murmu T. Thermo-mechanical vibration of FGM sandwich beam under variable elastic foundation using differential quadrature method. J Sound Vib 2008. doi:10.1016/j.jsv.2008.09.018.
[24] Y.-W. Kim, Temperature dependent vibration analysis of functionally graded rectangular rplates,J.SoundVib.284(2005)531–549.
[25] S.Kitipornchai,J. Yang,K. M.Liew, Random vibration of the functionally graded laminates in thermal environments, Comput. MethodsAppl.Mech.Eng.195(2006)1075–1095.
[26] Q.Li,V. P.Iu, K.P.Kou, Three-dimensional vibration analysis of functionally graded material plates in thermal environment, J.SoundVib.324(2009)733–750.
[27] J.N. Reddy, C.D.Chin, Thermomechanical analysis of functionally graded cylinders and plates, J.Therm. Stresses 21(1998)593–626.
[28] H.S.Shen, Nonlinear bending response of functionally graded plates subjected to transverse load sand in thermal environments, Int.J.Mech.Sci.44(2002)561–584.
[29] P.Shi,C. Y.Dong, Vibration analysis of functionally graded annular plates with mixed boundary conditions in thermal environment, J.SoundVib.331(2012)3649–3662.
[30] Delale F, Erdogan F. The crack problem for a nonhomogeneous plane. ASME J Appl Mech 1983;50:609–14.
[31] Bao G, Wang L. Multiple cracking in functionally graded ceramic/metal coatings. Int J Solids Struct 1995;32:2853–71.
[32] Cubberly, W. H. (1989). Metals Handbook 9th ed: ASM.
[33] Munro, R. G. (1997). Evaluated Material Properties for a Sintered α-Alumina. Journal of the American Ceramic Society, 80(8), 1919-1928.
[34] J. N. Reddy & C. D. Chin (1998): Thermo-mechanical analysis of functionally graded cylinders and plates, Journal of Thermal Stresses, 21:6, 593-626